

bradscholars

Microscopic biological cell level model using modified finite-difference time-domain at mobile radio frequencies

Item Type	Article
Authors	See, Chan H.;Abd-Alhameed, Raed;Excell, Peter S.;Zhou, Dawei
Citation	See CH, Abd-Alhameed R, Excell PS et al (2008) Microscopic biological cell level model using modified finite-difference time-domain at mobile radio frequencies. PIERS Online. 4(1): 6-10.
Rights	© 2008 PIERS. Reproduced in accordance with the publisher's self-archiving policy.
Download date	2026-04-14 21:49:59
Link to Item	http://hdl.handle.net/10454/815

The University of Bradford Institutional Repository

This work is made available online in accordance with publisher policies. Please refer to the repository record for this item and our Policy Document available from the repository home page for further information.

To see the final version of this work please visit the publisher's website. Where available, access to the published online version may require a subscription.

Author(s): See, C.H., Abd-Alhameed, R.A., Excell, P.S. and Zhou, D.

Title: Microscopic biological cell level model using modified finite-difference time-domain at mobile radio frequencies

Publication year: 2008

Journal title: PIERs Online

ISSN: 1931-7360

Publisher: PIERs

Publisher's site: <http://piers.mit.edu/piersonline/>

Link to original published version:

<http://piers.mit.edu/piersonline/download.php?file=MDcwOTA1MDYwOTI0fFZvbDRObzFQYWdlNnRvMTAucGRm>

Copyright statement: © 2008 PIERs. Reproduced in accordance with the publisher's self-archiving policy.

Microscopic Biological Cell Level Model Using Modified Finite-difference Time-domain at Mobile Radio Frequencies

C. H. See, R. A. Abd-Alhameed, P. S. Excell, and D. Zhou

Mobile and Satellite Communications Research Centre, University of Bradford
Richmond Road, Bradford, West Yorkshire, BD7 1DP, UK

Abstract— The paper demonstrates the modelling of the interaction mechanism between the biological tissues and electromagnetic field at mobile communication frequency ranges. The implementing of modified FDTD numerical method using frequency scaled FDTD with Floquet periodic boundary conditions and modified PMLs, the microdosimetric modelling of bioelectromagnetic interactions at cellular level, is established. In order to include the membrane effect on the biological tissues model in the analysis, the LE-FDTD is exploited to embed the lumped element cell-membrane model on the surface of the proposed tissue model in the FDTD computational domain. A new different structures of biological tissues are modeled and discussed, this includes a cluster of cylindrical cells. In order to imitate the effect of periodic replication of assemblages, Floquet periodic boundary conditions are imposed on the proposed model. Thus, the analysis of a large structure of cells is made more computationally efficient than the modeling of the entire structure. The total field distributions were shown in the context.

1. INTRODUCTION

The interest in diagnostic and therapeutic applications of RF/microwaves in Medicine and in the assessment of possible health hazards due to EM radiation have stimulated the development of research streams in both modelling and experiments for evaluating EM power deposition in the interior of the human body or biological system. In order to establish precisely the required safety standard for regulating human exposure to EM waves, different aspects of studying the problem such as tissue level [1–6], cell level [7] and ionic level [8] have been carried out theoretically and experimentally. In this particular research area, the Finite-Difference Time-Domain (FDTD) method has been a overwhelming majority of the numerical techniques to solve various of different electromagnetic problem due to its simplicity and capable to handle complex geometry.

This paper is devoted to investigate the EM field distribution over the new proposed cylindrical cells equivalent tissue model by using modified FDTD numerical technique. Different EM approaches have been used to analyze this problem, in particular, the lumped-element FDTD has been implemented to model the cell's membrane. This was achieved with the use of Hodgkin-Huxley (HH) model and the Floquet theorem, in order to mimic the infinite model of the tissue and in turn to reduce the computational time. Due to the analysed structure under consideration is considerably smaller than the wavelength of mobile communication frequency GSM900/GSM1800 and also the time steps required for GSM900/GSM1800 frequency involves some millions of iterations, therefore, quasi-static FDTD is exploited to perform the computation of the analysis. The electric field distribution along the centre of the analysed various structures are discussed in which the computational results are found in well agreement with the previous published results [4, 6].

2. SUMMARY OF THE METHOD

Figure 1 shows a simple geometry for the elucidation of three-dimensional periodic boundary implementation. As can be observed, the periodic boundaries are imposed on the x - and y -sides of the structures, while modified Absorbing Boundary Conditions (ABCs) [6] are applied to truncate the space lattice along z -axis. The coordinate points (i_o, j_o, k_o) and (i_N, j_M, k_p) denote a space point in a uniform rectangular lattice, where i_o, j_o, k_o are the smallest lattice grid number in x, y, z direction respectively and i_N, j_M, k_p are the largest lattice grid number in x, y, z direction respectively.

Consider the problem space is filled with the lossless medium ($\sigma = 0, \epsilon_o \epsilon_r$ and $\mu = \mu_o$) and normal incident plane wave is propagating along z axis. The tangential electric fields distribution on plane i_o, i_N, j_o and j_M are illustrated in Fig. 2. As can be seen, the red arrows are representing the tangential electric field components which are located on edge of the surface plane, while the

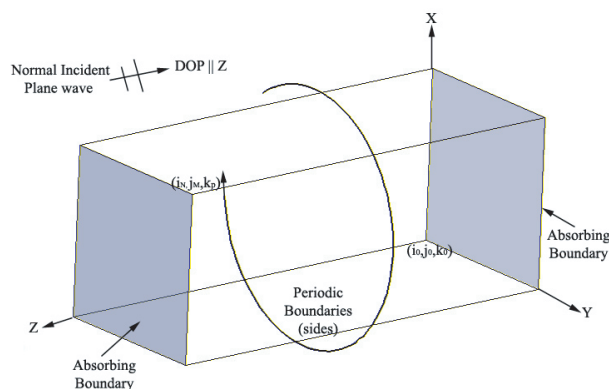


Figure 1: Geometry used in the analysis of 3-D infinite periodic structure illuminated by a normal incident plane wave.

black arrows are indicated as the rest of the tangential electric field components which are located on the surface plane. It should be noted that the explanation of the implementation method of the periodic boundary condition into FDTD computation domain in the following context, are based on the normal incidence methods [9, 10], therefore, it is only applicable when the normal incidence plane wave is used. For the sake of simplicity and consistency of explanation of updating equations for the periodic boundary condition on the surfaces of the geometry shown in Fig. 1, the updating equations of the tangential electric components (E_x , E_z and E_y) which are not on the edge of the surface will be firstly to be discussed, and subsequently, the updating equations of the edged tangential electric component (E_z) are demonstrated.

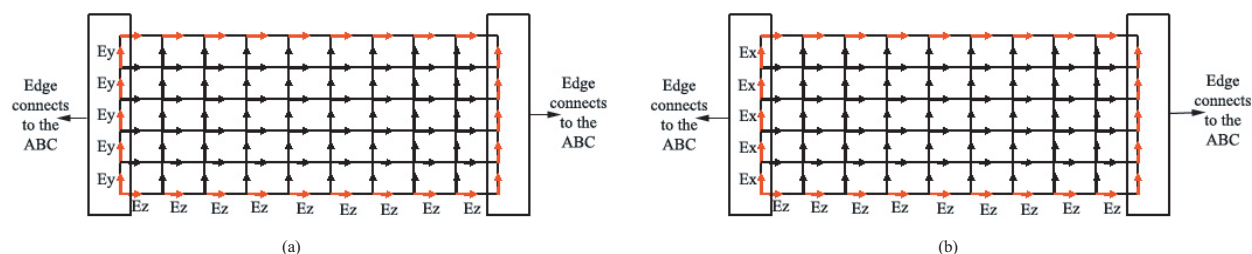


Figure 2: (a) Location of $E_z(\rightarrow)$ and $E_y(\uparrow)$ components in plane $i = i_0$ and i_N , (b) Location of $E_z(\rightarrow)$ and $E_x(\uparrow)$ components in plane $j = j_0$ and j_M .

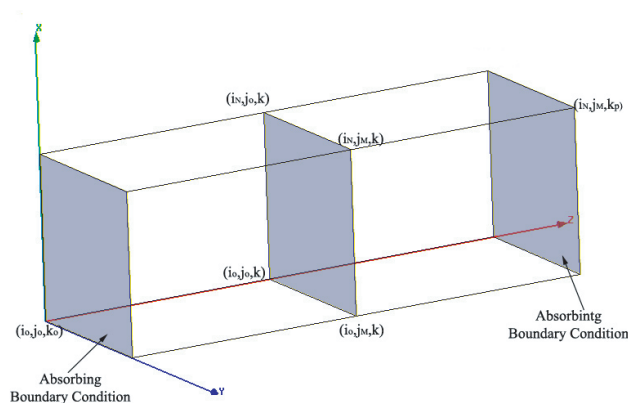


Figure 3: Location of the edged tangential component (E_z).

Consider the four surfaces planes at $i = i_0, i_N$ and $j = j_0, j_M$, in which the floquet periodic boundary condition should be applied as shown in Fig. 1. From Fig. 2(a), the 3D updating equations for the tangential electric components (E_y and E_z) which are not located on the edge of surface

plane $i = i_0$ and i_N , can be stated in the following forms:

$$E_y^{n+1}(i, j, k) = E_y^n(i, j, k) + \frac{\Delta t}{\varepsilon \Delta} \left(\begin{array}{l} H_x^{n+\frac{1}{2}}(i, j, k + 1/2) - H_x^{n+\frac{1}{2}}(i, j, k_p - 1/2) \\ + H_z^{n+\frac{1}{2}}(i - 1/2, j, k) - H_z^{n+\frac{1}{2}}(i + 1/2, j, k) \end{array} \right) \quad (1)$$

$$E_y^{n+1}(i_N, j, k) = E_y^{n+1}(i, j, k) \quad (2)$$

$$E_z^{n+1}(i, j, k) = E_z^n(i, j, k) + \frac{\Delta t}{\varepsilon \Delta} \left(\begin{array}{l} H_y^{n+\frac{1}{2}}(i + 1/2, j, k) - H_y^{n+1/2}(i_N - 1/2, j, k) \\ + H_x^{n+\frac{1}{2}}(i, j - 1/2, k) - H_x^{n+\frac{1}{2}}(i, j + 1/2, k) \end{array} \right) \quad (3)$$

$$E_z^{n+1}(i_N, j, k) = E_z^{n+1}(i, j, k) \quad (4)$$

where Δt is the time increment and Δ is the space lattice increment.

As for the 3-D updating equations for the tangential components (E_x and E_z) which are not located on the edge of the surface at plane $j = j_0$ and j_M as shown in Fig. 2(b), can be derived as follows:

$$E_x^{n+1}(i, j, k) = E_x^n(i, j, k) + \frac{\Delta t}{\varepsilon \Delta} \left(\begin{array}{l} H_z^{n+\frac{1}{2}}(i, j + 1/2, k) - H_z^{n+\frac{1}{2}}(i, j_M - 1/2, k) \\ + H_y^{n+\frac{1}{2}}(i, j, k - 1/2) - H_y^{n+\frac{1}{2}}(i, j, k + 1/2) \end{array} \right) \quad (5)$$

$$E_x^{n+1}(i, j_M, k) = E_x^{n+1}(i, j, k) \quad (6)$$

$$E_z^{n+1}(i, j, k) = E_z^n(i, j, k) + \frac{\Delta t}{\varepsilon \Delta} \left(\begin{array}{l} H_y^{n+\frac{1}{2}}(i + 1/2, j, k) - H_y^{n+1/2}(i - 1/2, j, k) \\ + H_x^{n+\frac{1}{2}}(i, j_M - 1/2, k) - H_x^{n+\frac{1}{2}}(i, j + 1/2, k) \end{array} \right) \quad (7)$$

$$E_z^{n+1}(i, j_M, k) = E_z^{n+1}(i, j, k) \quad (8)$$

As for the case of the edged tangential electric components (E_x , E_y , E_z) on plane $i = i_0$, i_N and $j = j_0$, j_M , and due to the E_x and E_y components are on the edge of the absorbing boundary conditions as shown in Fig. 2(a) and (b), therefore, they are assumed to be updated by the ABC updating equations. It should be noted that the only edged E_z tangential components will be considered here for the periodic boundary condition. According to Fig. 3, due to the presence of normal incidence plane wave, hence, four equations of E_z tangential components can be updated simultaneously. This can be simply done by using the following modified updated equations:

$$E_z^{n+1}(i, j, k) = E_z^n(i, j, k) + \frac{\Delta t}{\varepsilon \Delta} \left(\begin{array}{l} H_y^{n+\frac{1}{2}}(i + 1/2, j, k) - H_y^{n+1/2}(i_N - 1/2, j, k) \\ + H_x^{n+\frac{1}{2}}(i, j_M - 1/2, k) - H_x^{n+\frac{1}{2}}(i, j + 1/2, k) \end{array} \right) \quad (9)$$

$$E_z^{n+1}(i_N, j_M, k) = E_z^{n+1}(i, j, k) \quad (10)$$

$$E_z^{n+1}(i_N, j_M, k) = E_z^{n+1}(i, j, k) \quad (11)$$

$$E_z^{n+1}(i_0, j_M, k) = E_z^{n+1}(i, j, k) \quad (12)$$

$$(13)$$

3. SIMULATION AND RESULTS

A stack of ten cylindrical cells was investigated, as shown in Fig. 4. The radius and height of the each cell were considered to be 10 μm and 20 μm respectively. A plane wave of 100 V/m, propagating in the z -direction and polarized in the x -direction was used as excitation source. Note that the incident plane wave excitation was applied on a plane lying between the PML region and the outer limit of the FDTD grid. The PML, shown in Fig. 4, was 6 FDTD elements wide, the grading factor g was 10.1383 and the grid structure was effectively extended to infinity in the x - and y -directions, by imposing the Floquet boundary condition along the x and y axes. The Floquet periodic boundary condition plays an important role to mimic the presence of an extended 3-dimensional structure of biological cells, simulating connected tissue. The FDTD problem space was $220 \times 20 \times 20$ FDTD elements of size 1 μm while a discretization time step δt of 1.3 femtoseconds was chosen to drive the FDTD computation, to meet the requirements of the Courant stability criterion.

The shape of the living cells can be so diverse. In order to have better understanding on the effects of EM field interaction with different geometries of biological tissues, a cluster of such

cylindrical cells model of the tissue is proposed for the present work. This analysis is performed in which the material properties unchanged as in the case of spherical and cubical cell structures, as in [6]. Fig. 5 describes the 2D view of electric field distribution of the proposed cylindrical-cell tissue at 10 GHz, while the electric field distribution along the centre of the analysed structure is shown in Fig. 6, where the Fig. 7 are the amplified version of the Fig. 6.

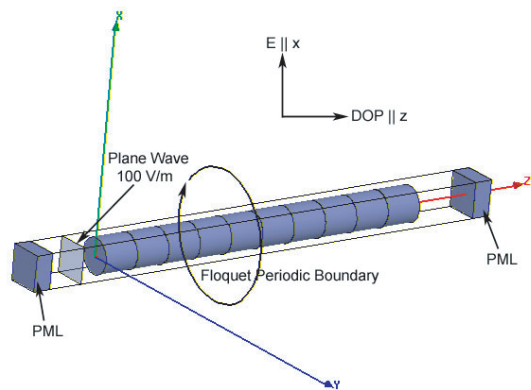


Figure 4: The three-dimensional view of the simulated cubical structures in FDTD computational domain.

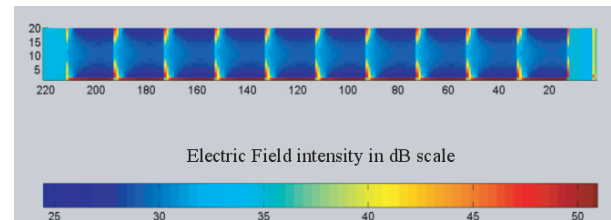


Figure 5: Modulus of the electric field on xz-plane at intermediate frequency 10 GHz (logarithmic scale).

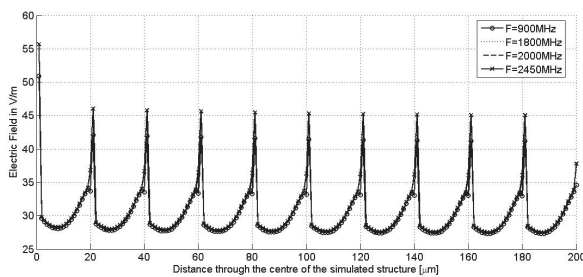


Figure 6: Penetration of electric field along z axis, through the centre of the simulated structure.

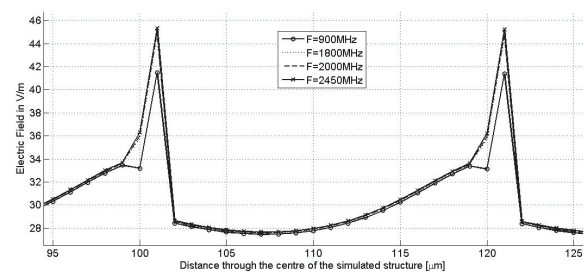


Figure 7: Penetration of electric field (enlargement of Fig. 5).

The loading effect of the HH model into the cylindrical-cell tissue has also been studied. Fig. 8 demonstrates the difference of 15% in field magnitude with and without the presence of HH model in the proposed simulated structure. The results show consistent difference with the previous spherical- and cubical-cells tissue simulated structures [6].

The comparison of the field distribution of spherical-, cubical- and cylindrical- cells tissue model, through the centre of the analysed structure, is elucidated in Fig. 9. The peak field on the membrane of the cylindrical structure is found to be about 1.7 times higher than in the cytoplasm, which is

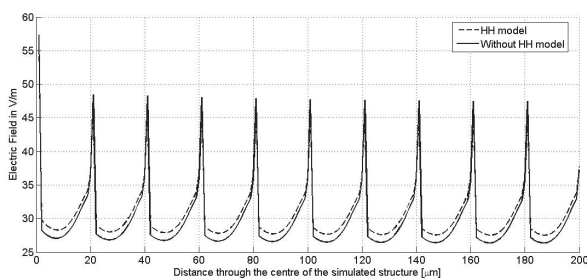


Figure 8: Electric field distribution along z -axis, through the centre of the simulated cubical-cell structure in Fig. 3, incorporating Hodgkin-Huxley model and driven at 2400 MHz.

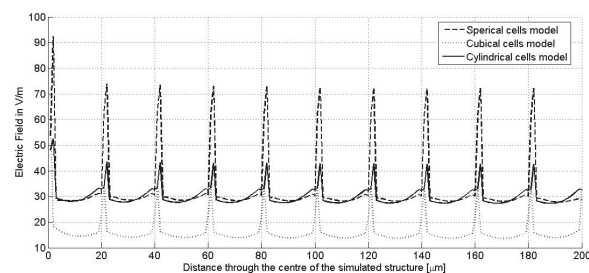


Figure 9: Comparison of field values of three different simulated structures at 900 MHz.

distinct with the previous two models [6]. As can be noticed, the peak field value of this cylindrical model is higher than the cubical model and lower than the spherical model, whereas the peak field value on the cytoplasm is the about the same as in the spherical model and double the value found in the cubical structure.

4. CONCLUSIONS

The combination of quasi-static FDTD, an arbitrarily-oriented lumped element membrane model, the modified Berenger's absorbing boundary condition and the Floquet periodic boundary condition represent a significant advance in verisimilitude of biological cell modeling, is demonstrated. By adopting the proposed methodology, it permits the computationally-efficient FDTD method to model small cell size object with reasonable computing time and accuracy.

REFERENCES

1. Gandhi, O. P. and J. Chen, "Numerical dosimetry at power-line frequencies using anatomically based models," *Bioelectromagnetics*, Vol. 13, 43–60, 1992.
2. Gandhi, O. P., G. Lazzi, and C. M. Furse, "Electromagnetic absorption in the human head and neck for mobile telephones at 835 and 1900 MHz," *IEEE Transactions on Microwave Theory and Techniques*, Vol. 44, 1884–1896, 1996.
3. Kotnik, T. and D. Miklavcic, "Theoretical evaluation of the distributed power dissipation in biological cells exposed to electric fields," *Bioelectromagnetics*, Vol. 21, 385–394, 2000.
4. Emili, G., A. Schiavoni, F. L. Roselli, and R. Sorrentino, "Computation of electromagnetic field inside a tissue at mobile communications frequencies," *IEEE Transactions on Microwave Theory and Techniques*, Vol. 51, 178–186, 2003.
5. Hadjem, A., D. Lautru, C. Dale, M. F. Wong, V. F. Hanna, and J. Wiart, "Study of Specific Absorption Rate (SAR) induced in two child head models and in adult heads using mobile phones," *IEEE Transactions on Microwave Theory and Techniques*, Vol. 53, 4–11, 2005.
6. See, C. H., R. A. Abd-Alhameed, and P. S. Excell, "Computation of electromagnetic fields in assemblages of biological cells using a modified finite difference time domain scheme," *IEEE Transactions on Microwave Theory and Techniques*, No. 55, 1986–1994, Sept 2007.
7. Martin, S. M. S., J. L. Sebastian, M. Sancho, and J. M. Miranda, "A study of the electric field distribution in erythrocyte and rod shape cells from direct RF exposure," *Phys. Med. Biol.*, Vol. 48, 1649–1659, 2003.
8. Apollonio, F., M. Liberti, and G. D'Inzeo, "Theoretical evaluation of GSM/UMTS electromagnetic fields on neuronal network response," *IEEE Transactions on Microwave Theory and Techniques*, Vol. 50, 3029–3035, 2002.
9. Taflove, A. and S. C. Hagness, *Computational Electrodynamics: The Finite-Difference Time-domain Method*, 2nd ed, Artech House, Inc, 2000.
10. Alexanian, A., N. J. Koliass, R. C. Compton, and R. A. York, "Three-dimensional FDTD analysis of quasi-optical arrays using Floquet boundary conditions and Berenger's PML," *IEEE Microwave and Guided Wave Letters*, No. 6, 138–140, 1996.